ATRX alteration contributes to tumor growth and immune escape in pleomorphic sarcomas

Lucie Darmusey[1,2,3]*, Gaëlle Pérot[1,4]*, Noémie Thébault[1,2], Sophie Le Guellec[1,2], Nelly Desplat[5], Laëtitia Gaston[6], Lucile Delespaul[1,8], Tom Lesluyes[1,8], Elodie Darbo[5,7,8], Anne Gomez-Brouchet[1,2,4], Elodie Richard[5], Jessica Baud[5], Laura Leroy[1,2], Jean-Michel Coindre[5,9], Jean-Yves Blay[10,11], Frédéric Chibon[1,2,5]

1. OncoSarc, INSERM U1037, Cancer Research Center in Toulouse (CRCT), Toulouse, France.
2. Department of Pathology, Institut Claudius Régaud, IUCT-Oncopole, Toulouse, France.
3. University of Toulouse 3, Paul Sabatier, Toulouse, France.
4. Centre Hospitalier Universitaire (CHU) de Toulouse, IUCT-Oncopole, Toulouse, France.
5. INSERM UMR1218, ACTION, Institut Bergonié, Bordeaux, France.
6. Department of Medical Genetics, CHU de Bordeaux, Bordeaux, France.
7. CNRS UMR5800, LaBRI, Talence, France.
8. University of Bordeaux, Bordeaux, France.
9. Department of Pathology, Institut Bergonie, Bordeaux, France.
10. Department of Medical Oncology, Centre Léon Bérard, Lyon, France.
11. University Claude Bernard Lyon 1, Inserm U1052, CNRS 5286, Cancer Research Center of Lyon, Lyon, France.
* These authors contributed equally

Running title: In pleomorphic sarcoma ATRX loss allows immune escape

Key words: Sarcomas, ATRX, oncogenesis, mast cells, alteration

Corresponding author: Frédéric Chibon, Cancer Research Center in Toulouse (CRCT), 2 avenue Hubert Curien, 31037, Toulouse, France, 0582741765, Frederic.chibon@inserm.fr

Financial support: The Instituts Thematiques Multiorganismes (ITMO) Cancer and the International Cancer Genome Consortium supported this work.

Conflict of interest: The authors declare no potential conflicts of interest.

Note: L. Darmusey and G. Pérot contributed equally to this work

Authors' Contributions:
Conception and design: L. Darmusey, G. Pérot, N. Thébault, F. Chibon
Development of methodology: L. Darmusey, G. Pérot, N. Thébault, F. Chibon
Acquisition of data (provided animals, acquired and managed patients, provided facilities, etc.): L. Darmusey, G. Pérot, N. Thébault, S. Le Guellec, N. Desplat, L. Gaston, L. Delespaul, T. Lesluyes, E. Darbo, A. Gomez-Brouchet, E. Richard, J. Baud, L. Leroy
Analysis and interpretation of data (e.g., statistical analysis, bio-statistics, computational analysis): L. Darmusey, G. Pérot, N. Thébault, F. Chibon
Writing, review, and/or revision of the manuscript: L. Darmusey, G. Pérot, N. Thébault, F. Chibon
Administrative, technical, or material support (i.e., reporting or organizing data, constructing databases): J.M. Coindre, J.Y. Blay
Study supervision: F. Chibon
Other (data, expertise, and guidance): The French Sarcoma Group and the International Cancer Genome Consortium

Abstract:

Whole genome and transcriptome sequencing of a cohort of 67 leiomyosarcomas revealed *ATRX* to be one of the most frequently mutated genes in leiomyosarcomas after *TP53* and *RB1*. While its function is well described in the alternative lengthening of telomeres mechanism, we wondered whether its alteration could have complementary effects on sarcoma oncogenesis. *ATRX* alteration is associated with the down-expression of genes linked to differentiation in leiomyosarcomas, and to immunity in an additional cohort of 60 poorly differentiated sarcomas. *In vitro* and *in vivo* models showed that *ATRX* loss increases tumor growth rate and immune escape by decreasing the immunity load of active mast cells in sarcoma tumors. These data indicate that an alternative to unsuccessful targeting of the adaptive immune system in sarcoma could be to target the innate system. This might lead to a better outcome for sarcoma patients in terms of *ATRX* status.

Statement of significance:

There is still no efficient systemic treatment for pleomorphic sarcomas. Here we show that 1/4 of them have an ATRX alteration that diminishes the immune response. This phenotype is related to the inhibition of mast cell recruitment upon ATRX alteration, which could be targeted to adapt immunotherapy against pleomorphic sarcomas.

Introduction:

Pleomorphic sarcomas are a group of rare mesenchymal tumors comprising different histotypes such as undifferentiated pleomorphic sarcoma (UPS), myxofibrosarcoma (MFS), dedifferentiated liposarcoma (DDLPS), osteosarcoma (OS) and leiomyosarcoma (LMS), which is the most frequent subtype (1). LMS has a smooth muscle differentiation and can occur in any anatomical site, although there are three main locations: limbs, trunk and uterus. Currently, the first-line treatment is wide-margin resection for localized tumors and anthracycline-based chemotherapy for advanced tumors (2). However, these treatments are still not effective enough as 48 to 89% of LMS develop metastases depending on the tumor location and the mortality rate is between 50 and 65% with a median survival of around 12 months (3,4). From a genomic standpoint, LMS, like other pleomorphic sarcomas, have a very rearranged and unbalanced karyotype (2).

In a whole genome and whole transcriptome sequencing study conducted by our team, Darbo *et al.* showed that LMS could be separated into two groups with specific clinical, transcriptomic and genomic features: the homogenous and the other LMS. Those groups share a low somatic mutation burden and a high level of copy-number alterations (Darbo *et al.*, 2020). But only three genes came out to be recurrently mutated (considering point mutations only), as also showed by the TCGA study (5): *TP53*, *RB1* and *ATRX* (mutated in 48.7%, 17.9% and 12.8% respectively). *RB1* (6,7) and *TP53* (8,9) are tumor suppressor genes that have long been known to be implicated in the oncogenesis of pleomorphic sarcomas. *ATRX* is a chromatin modifier gene with a Swi/Snf2 domain (10). Its tumor suppressive function has so far been related to its role in the alternative lengthening of telomeres (ALT) mechanism (11), inducing genome instability (12) and leading to a poor prognosis of *ATRX*-altered tumors (13). Recently, its involvement in senescence (14) and in intrinsic immunity *via* its interactions within promyelocytic leukemia nuclear bodies (PML NBs) (15) was questioned. Here, we investigated

whether ATRX might have additional impacts in the oncogenesis of pleomorphic sarcomas beyond its role in the ALT mechanism and show how its involvement in oncogenesis is also linked to differentiation, tumor growth and immunity.

Results:

Distinct genetic alterations trigger loss of ATRX protein

Sixty-seven LMSs (Cohort 1; Supplementary Table 1) were sequenced at the whole genome and transcriptome levels (28 LMSs + 39 LMSs from Darbo *et al*., 2020) and *ATRX* was identified as the third most frequently mutated gene after *TP53* and *RB1*. By integrating point mutations and structural variations (SV), ATRX is altered in 20 cases (29.8 %; Figure 1), with 8 point mutations (missense (MS) and non-sense (NS); 40%), 7 frameshifts (FS; 35%) and 5 structural variants (SV; 25%). All mutations and SVs were validated by an independent technique (RNA sequencing and/or Sanger sequencing) (Supplementary Tables 2 and 3; Supplementary Figures 1, 2, and 3). *ATRX* was altered in 23.7% of non-uterine LMSs (14/59) compared to 75% of uterine LMSs (6/8) , which is significantly higher in this specific anatomical site ($P = 7.002 \times 10^{-3}$; Figure 2A and Supplementary Figure 4). Altered cases were not enriched in any other clinical annotation (*i.e*. grade, metastasis or sex). Regarding SV, 3 out of 5 led to a loss of *ATRX* expression and the other two led to a frameshift (Supplementary Table 2). These alterations were hemizygous in the three males due to the location of *ATRX* on chromosome X (Xq21), and in two females with either a deletion of the second allele (LMS69) or an isodisomy (LMS49). In the other 15 females, 93.3% of the alterations (14/15) occurred on the active X, as RNAseq analysis showed the altered transcript expression (Supplementary Table 2). No expression of the mutated allele was detected in LMS48 (Supplementary Table 2 and Figure 2). Alterations were distributed throughout the whole gene but two regions were most frequently affected: one between exons 17 and 21 (40%, 6/15) and the other in exon 9

(33.4%, 5/15). At the mRNA level, mutated cases had a significantly lower *ATRX* expression than wild-type (WT) tumors ($P = 3.79 \times 10^{-4}$; Figure 2B) and at the protein level, alterations led to a loss of nuclear protein ($P = 8.04 \times 10^{-10}$; Figure 2B and Supplementary Figure 5).

Is ATRX alteration linked to ALT mechanism?

Since *ATRX* loss is linked to the ALT phenotype (16), the ALT status of tumors was determined. Most LMS were ALT-positive (ALT+, 76.9%, 50/65) (Figure 2A and Supplementary Figure 6). Both *ATRX* alteration ($P = 6.49 \times 10^{-3}$) and ATRX protein loss ($P = 6.29 \times 10^{-3}$) were significantly associated with the ALT mechanism (Figure 2C). However, while all *ATRX*-altered cases were ALT+, most ALT+ cases were *ATRX* WT (64%, 32/50) with 93.3% of cases (28/30) expressing the protein in the nucleus (Figures 2A and 2C).

Is *ATRX* alteration associated with prognosis?

Neither *ATRX* status (altered or WT), mRNA expression (below or above defined cut-off, see material and methods section), protein localization (nuclear or absent), nor ALT phenotype (positive or negative) could split patients into two groups with significantly distinct prognoses (Supplementary Figure 7).

Which transcriptomic program is modified upon *ATRX* alteration?

Searching for the oncogenic impact of these *ATRX* alterations, we tested whether altered tumors had a distinct transcriptomic program and identified 340 and 219 genes significantly down- and up-expressed in the *ATRX*-altered group, respectively ($P < 0.05$; Figure 3A). Functional enrichment analysis (Figure 3A) showed that genes down-expressed were significantly involved in blood pressure, heart contraction and striated muscle contraction. These findings were strengthened when patients were grouped according to ATRX protein localization, since genes down-expressed upon protein loss were found to be involved in similar biological mechanisms, *i.e*. muscle system and contraction (Figure 3B).

As expected, clustering based on these 559 differentially expressed genes (Supplementary Figure 8A) revealed a group with a high percentage of *ATRX*-altered patients (75%, 15/20). Patients in this cluster had tumors that were enriched in uterine or "other" LMS type ($P = 3.49 \times 10^{-7}$; Supplementary Figure 8B) (Darbo *et al.*, 2020). "Other" LMS are less differentiated than "homogeneous" LMS and are thought to derive from fibroblasts rather than smooth muscle cells (SMCs) (Darbo *et al.*, 2020).

The association between enrichment of down-expressed genes linked to muscle system and of oLMS in ATRX altered tumors suggested that either *ATRX* alteration preferentially occurs in partially or undifferentiated cells, or that it may induce dedifferentiation. To explore these hypotheses, we studied the *ATRX* status in a second cohort comprising poorly differentiated pleomorphic sarcomas characterized by RNAseq.

What are *ATRX* alterations in poorly differentiated pleomorphic sarcomas?

RNA sequencing of 60 pleomorphic sarcomas (cohort 2; Supplementary Table 1) from a previously published cohort (17) was reanalyzed and 10 *ATRX*-altered tumors (16.7%) were identified (Supplementary Tables 2 and 4; Supplementary Figures 9 and 10). The types of alteration as well as their functional consequences were similar to those detected in cohort 1 (Figure 4A). Altered cases were not enriched in any annotation (*i.e.* histotype, tumor site, grade, metastasis or sex) (Figure 4B) but had a significantly lower mRNA expression of *ATRX* ($P = 3.62 \times 10^{-2}$; Figure 4C) and were significantly associated with ALT ($P = 7.27 \times 10^{-4}$; Figure 4D). *ATRX*-altered tumors did not have a distinct prognosis in cohort 2 (Supplementary Figure 11A), nor when the two cohorts are merged (Supplementary Figure 11B).

What are the transcriptomic modifications in poorly differentiated sarcomas upon *ATRX* alteration?

Functional enrichment analysis of differentially expressed genes showed that *ATRX* alteration induced the overexpression of 76 genes enriched in GO terms related to the metabolic process, and the down-expression of 506 genes enriched in GO related to immunity. The five most significantly enriched GO were (Figure 5) "T cell activation" ($P = 8.41 \times 10^{-19}$), "lymphocyte activation" ($P = 1.13 \times 10^{-17}$), "immune system process" ($P = 4.82 \times 10^{-16}$), "leukocyte activation" ($P = 1.58 \times 10^{-14}$) and "regulation of immune system process" ($P = 1.82 \times 10^{-14}$).

Results from both cohorts indicated that *ATRX* alteration is associated with differentiation and immunity. Since this is particularly relevant as immunotherapies are currently not efficient in sarcomas, we functionally tested the hypothesis that *ATRX* alteration might modify the anti-tumor immune response.

Does *ATRX* knock-down impact oncogenic features?

To functionally test the impact of *ATRX* alterations, three models of *ATRX* knock-down ($ATRX^{KD}$) were constructed: i) a model to evaluate tumor growth *in vitro* and *in vivo* in a human UPS cell line (IB106), ii) another to study immunity in immunocompetent mice (Balb/c) with a mouse poorly differentiated OS (K7M2; a sarcoma with very close genetics to UPS and LMS) and iii) a third to compare human and mouse, using a human OS cell line (MG63). These cell lines were infected by lentivirus with an *ATRX* shRNA. Western blot evidenced the successful extinction of ATRX in each cell line (Figure 6A). ALT analysis showed that *ATRX* shRNA did not change ALT status in any cell line (Supplementary Figure 12).

In vitro, a significant ($P < 0.0001$) increase in proliferation was observed in the UPS cell line IB106 $ATRX^{KD}$ but not in OS cell lines (K7M2 and MG63) (Figure 6B). Colonies formed in soft agar assay revealed that the mouse cell line K7M2 was unable to form any colony with or without ATRX expression. In contrast, there was a significant increase in colony number in human cell lines IB106 and MG63 upon *ATRX* down-expression, from a mean of 14 to 21

colonies ($P = 2.6 \times 10^{-3}$) and from 4 to 13 ($P = 1 \times 10^{-3}$), respectively (Figure 6C). Next, IB106 *ATRX*^{CT} (control) and *ATRX*^{KD} cells were subcutaneously grafted in 10 NSG mice each. A tumor grew in 6/9 *ATRX*^{CT} group and in 9/10 *ATRX*^{KD} group. Tumor growth rates were three-fold higher in *ATRX*^{KD} tumors (91.2 ±7.6 mm^3/day) than in *ATRX*^{CT} tumors (32.9 ±10.6 mm^3/day) ($P = 5 \times 10^{-4}$, Figure 6D).

Does ATRX alteration modify anti-tumor immune response?

The involvement of ATRX alteration in immune escape was tested by grafting K7M2 *ATRX*^{CT} and *ATRX*^{KD} cells in immunodeficient NSG mice and in immunocompetent Balb/c mice (N=15 for each group). Growth rate was not significantly increased upon ATRX knock-down in any hosts (Figure 7A). Tumor-free survival in *ATRX*^{CT} and in *ATRX*^{KD} models displayed no significant differences in immunodeficient NSG mice, whereas in immunocompetent Balb/c mice there was 53.4% (8/13) of tumor induction with K7M2 *ATRX*^{CT} *versus* 92.8% (13/14) with K7M2 *ATRX*^{KD}. Therefore, tumor-free survival was significantly poorer upon *ATRX* knock-down ($P = 9.7 \times 10^{-3}$; Figure 7B).

Differential gene expression analysis between *ATRX*^{KD} *vs ATRX*^{CT} K7M2 tumors in Balb/c mice revealed that 37 genes were down-regulated and 23 genes were overexpressed in *ATRX*^{KD} tumors (Figure 7C). The low number of genes precluded any functional enrichment analysis. Consequently, a String Protein Interaction (18) analysis was performed. Whereas no consistent clusters arose with up-regulated genes upon *ATRX* knock-down (Supplementary Figure 13), one emerged in down-regulated genes, with 12 proteins out of 37 linked to mast cell pathways (including *TPSB2* coding tryptase, a widely used mast cells marker) (Figure 7D).

Immunofluorescence against tryptase on the murine tumors previously processed in RNAseq showed that mast cells expressing tryptase represented a mean of 0.8% of total cells in *ATRX*^{CT} tumors, whereas they constituted 0.3% of *ATRX*^{KD} tumors ($P = 0.01$; Figure 7E). This

significant difference prompted us to assess whether the proportion of infiltrating mast cells in human sarcomas is also related to *ATRX* alteration and the absence of ATRX from the nucleus. In the LMS cohort, the only one fully characterized at every level, *TPSB2* was significantly under-expressed in *ATRX*-altered cases ($P = 1.9 \times 10^{-4}$; Figure 7F) and in tumors with no nuclear ATRX ($P = 0.02$; Figure 7G), which might indicate that there are fewer infiltrating mast cells in these human LMS.

Discussion:

This in-depth *ATRX* genetic analysis revealed that *ATRX* alteration likely affects a quarter of pleomorphic sarcomas, since it was found in 29.8% of LMS and in 16.7% of undifferentiated sarcomas (US). Cohort 2 is less deeply characterized (WGseq for cohort 1, RNAseq for cohort 2), so cases might be missed with this RNAseq-based screening (20.7% observed for UPS/MFS/DDLPS in TCGA (5)). The rate of alteration in LMS is consistent with the rate of 24% found by Chudasama and colleagues (19), but it is slightly higher than that generally observed in other LMS cohorts, which is around 16% (5,20,21), probably due to the exhaustiveness of WGseq. *ATRX* mutations were distributed across the entire gene, as previously observed (5,19,22,23). Three main factors link the two types of sarcomas in the present study: i) in females, all alterations except in LMS48 can be interpreted as occurring on the active X, ii) point mutations are more frequent (75% in LMS and 60% in US) than structural variations (25% in LMS and 40% in US), as previously observed (5,19); and iii) the alterations lead preferentially to a frameshift and thus to a truncated protein in 66.7% of cases (20/30, 65% in LMS and 70% in US), in agreement with previous descriptions in sarcomas (5,19,22,24). Of note, *ATRX* alterations in the present study were not significantly associated with a poorer prognosis. However, this association depends on the cohorts studied (13,23) and was observed in only one cohort that mainly included missense mutations (23).

ATRX mutated cases were also linked to the location of LMS, *i.e.* 75% of uterine cases were *ATRX*-altered (6/8). Loss of *ATRX* in uterine tumors is a key difference between benign and malignant tumors. In this location, it has been proposed to use *ATRX* loss as a marker of the highly probable evolution of benign tumors toward malignancy (25). In other LMS locations, ATRX loss is linked to the "other" LMS group. LMS belonging to this subtype are mainly poorly differentiated and likely originate from fibroblastic cells (Darbo *et al.*, 2020). Furthermore, as ATRX loss in LMS is associated with a lower expression of genes related to smooth muscle activity, we hypothesize that it occurs preferentially in poorly differentiated cells. The degree of cell differentiation may be crucial for the loss of ATRX to confer advantages to the precursor sarcoma cell.

ATRX knock-down modifies tumor cell proliferation, as confirmed *in vivo* where *ATRX* knock-down tumors grew three-fold faster than controls, and clonogenicity in sarcoma models. Interestingly, poorly differentiated sarcomas with *ATRX* alteration overexpressed genes related to metabolism, whose upregulation is a known hallmark of cancers and supports cell survival and proliferation (26). The hypothesis that ATRX could act through metabolism regulation is a very appealing one that now requires functional validation.

In vivo experimentation revealed a new role of ATRX, as its alteration was associated with a poorer outcome exclusively in an immunocompetent murine host, and with down-expression of immune-related genes in poorly differentiated human sarcomas. These two findings show that ATRX loss can influence the regulation of immune response in sarcomas, probably by limiting mast cell recruitment, as evidenced by the lower proportion of tumor infiltrating mast cells upon *ATRX* down-expression. The role of mast cells in tumor control is currently considered as dual and antagonistic, since they can support tumorigenesis or suppress tumor growth. Their role is dependent on the type of tumor (27). To our knowledge, no study has yet investigated the role of mast cells in the oncogenesis of sarcomas. *FcεRI* and *Ms4a2* are two

down-expressed genes in *ATRX*^{KD} K7M2 tumors. They are part of the IgE activating mast cell pathway that confers them a protective role in epithelial tumors (28). In addition to their higher proportion, these mast cells present in *ATRX*^{WT} tumors likely play a suppressor role in which they recruit other immune cells to tumor sites by enhancing vascular permeability and direct chemoattraction (29). In human LMS, the absence of ATRX is linked to the down-expression of *TPSB2*, which is a protein produced almost exclusively by mast cells and widely used to identify them. Furthermore, genes down-expressed by *ATRX*-altered poorly differentiated sarcomas are mostly linked to adaptive immune cell activation, so adaptive immune cells are either less present or less active. This could be achieved by avoiding the release of chemoattractants and hence the recruitment or activation of other immune cells. The precise mechanism involved upon ATRX loss that changes the immune microenvironment of sarcomas needs to be deciphered.

Regarding *ATRX* expression, 27% of cases (17/63) showed no nuclear ATRX protein, which is consistent with the literature (13,22,23,30). In tumors presenting FS/NS, 87.5% (14/16) exhibited no ATRX protein at all. In these cases, *ATRX* mRNA level was low, likely meaning that if the truncated protein is expressed (missed by our screening with the C-terminal antibody), it should be very low. Moreover, if truncated proteins are expressed, the lost domains should be the same in all studied sarcoma types, with partial or complete loss of the helicase C-terminal domain in 90% of cases (18/20) and of both helicase domains in 70% of cases (14/20). As the majority of MS mutations occurred in one helicase domain (71.4%, 5/7) and IHC detected a nuclear localization of the protein, a decrease in ATRX enzymatic activity may be hypothesized (31). Collectively, these results suggest that alterations of *ATRX* preferentially target its enzymatic functions rather than its protein-protein interactions, thus explaining why mutations in *ATRX* partner genes (*i.e. DAXX*, *EZH2*, *SP100*) are not frequent and not an alternative to *ATRX* alteration in sarcomas. We thus hypothesize that, by modifying its

chromatin remodeling action, alterations of *ATRX* trigger a specific transcriptomic program that promotes attenuated mast cell recruitment, leading to the observed immune response in models and human tumors.

Our findings show that *ATRX* alterations are quite frequent in pleomorphic sarcomas (close to 25%) and mostly lead to the loss of ATRX. In addition, they demonstrate that *ATRX* alterations are not only associated with ALT phenotype but also with differentiation and immune response regulation through non-recruitment of mast cells. Currently, most immunotherapies of sarcomas, which target the adaptive immune system and specifically T cells by helping them to recognize tumors, have a low response rate (32). Indeed, several recent trials have assessed the response to checkpoint inhibitors, which are used to thwart immune system escape by activating CD8+ cytotoxic T cells, with an overall response rate not higher than 25% (33,34). A better response rate with around 66% of response was reached by transferring autologous T cells transduced with a T cell receptor directed against a cancer antigen (CAR-T cell) expressed by the selected tumors, but only 6 patients were involved (35). As targeting the adaptive immune system does not work well in sarcomas, some have tried to target the innate immune system by making therapeutic vaccines which rely on the activation of dendritic cells in the presence of predetermined immunogenic antigen (32). One trial presented 10 out of 23 patients who lived more than 1 year whereas others died after around 7 months (36) and another one showed a 1-year progression-free survival of 70.6% (37). Targeting the innate system might therefore lead to a better outcome for sarcoma patients that could be further improved by assessing *ATRX* status before testing mast cell-enhancing therapies, as they have been successful in other solid tumors (38). These therapies enhanced local mast cells degranulation by using IgE antibodies, as proposed by Singer and Jensen-Jarolim (39). This strategy could be useful in $ATRX^{WT}$ tumors to enhance the anti-tumoral action of mast cells and, in *ATRX*-altered sarcomas, to enhance mast cell recruitment and activation (40).

Material and Methods:

Collection of samples and access to data

Samples used in cohort 1 were collected prospectively by the French Sarcoma Group as part of the ICGC program (International Cancer Genome Consortium). Samples used in cohort 2 were part of the cohort used in Lesluyes *et al.* (2016). ICGC Whole-Genome sequencing and RNA sequencing data for the 67 LMS are available at https://dcc.icgc.org/projects/LMS-FR.

Tumor samples and histological classification

One hundred and twenty-seven soft tissue sarcomas were selected according to their histological subtype. Cases were obtained from the collective database of the French Sarcoma Group (https://conticabase.sarcomabcb.org). All cases were systematically reviewed by expert pathologists of the French Sarcoma Group according to the World Health Organization guidelines (41). As such, tumors were classified into four categories: leiomyosarcomas (n=67), undifferentiated pleomorphic sarcomas (n=30), myxofibrosarcomas (n=17) and dedifferentiated liposarcomas (n=13) (Supplementary Table 1). Clinico-pathological data and patient information are summarized in Supplementary Table 1. The 67 leiomyosarcomas are part of the ICGC program (International Cancer Genome Consortium) (cohort 1). Constitutional DNA and tumor DNA and RNA were available for these cases. For the other cases (cohort 2), only tumor DNA and RNA were available.

Validation of *ATRX* alterations

For cohort 1, all FS were verified at both DNA and RNA levels by Sanger sequencing. All SV were verified on DNA by Sanger sequencing and the effect on RNA was detected by RNAseq. Regarding MS and NS mutations, only those not found in both WG-seq and RNAseq were verified by Sanger sequencing. Complete deletion of *ATRX* due to total loss of chrXq or chrX

was seen in 4 females all presenting RNA expression and nuclear protein, implying that the loss occurred on the inactive X. One triploid tumor developed in a male also presented a deletion of the gene but with one copy left. Therefore, they were all considered as WT regarding *ATRX* alteration. For cohort 2, whole *ATRX* cDNA was sequenced by Sanger sequencing for all cases and alterations found at RNA level were verified on DNA.

PCR on genomic DNA

For screening of mutations on genomic DNA, PCR primers were designed using the Primer 3 program (http://frodo.wi.mit.edu/primer3/) and are presented in Supplementary Table 5. All PCR were performed on 50ng of DNA using AmpliTaqGold® DNA polymerase (4311820, Applied Biosystems, Foster City, CA, USA) according to the manufacturer's instructions with the PCR program described in the Supplementary Table 5 Legend.

RT-PCR

Total RNA was first reverse-transcribed using random hexamers and the High Capacity cDNA Reverse Transcription Kit (4368814, Applied Biosystems, Foster City, CA, USA) according to the manufacturer's instructions. All primers used were designed using the Primer 3 program (http://frodo.wi.mit.edu/primer3/). For *ATRX* cDNA screening, primers used are presented in Supplementary Table 6. For fusion transcript detection, control PCR were first performed with different forward and reverse primers for each gene implicated in the fusion, and then PCR was performed using a forward primer for one gene and reverse primer for the other gene (Supplementary Table 7). All PCR were performed as previously described for PCR on genomic DNA.

Sanger Sequencing

PCR products were purified using an ExoSAP-IT PCR Purification Kit (US78200, GE Healthcare, Piscataway, NJ, USA) and sequencing reactions were performed with the Big Dye

Terminator V1.1 Kit (4336805, Applied Biosystems, Foster City, CA, USA) according to the manufacturer's recommendations. Samples were purified using the Big Dye XTerminator Purification kit (4376486, Applied Biosystems, Foster City, CA, USA) according to the manufacturer's instructions and sequencing was performed on a 3730xl Genetic Analyzer for cohort 1 or 3130xl Genetic Analyzer for cohort 2 (Applied Biosystems, Foster City, CA, USA). Sequences were then analyzed using the Sequencing analysis V5.3.1 and the SeqScape V2.6 software (Life Technologies, Carlsbad, CA, USA). FinchTV software (V1.4.0) was also used (Geospiza, Seattle, WA, USA).

Immunohistochemistry

Sixty-seven tumors in cohort 1 were analyzed on tissue microarrays. Each case was represented by three spots 4-µm-thick and 1mm in diameter. Immunohistochemistry was performed on a BenchMark Ultra instrument (Ventana, Washington D.C, USA). Antigen retrieval was performed using a CC1 protocol for 16 min at 98°C (Ventana, Washington D.C, USA), and the anti-ATRX antibody (1:1000, Clone BSB-108, Diagomics, Blagnac, France) was diluted in PREPKIT9 for 20 min. Antibody detection was performed using the Optiview detection kit (860-099, Ventana, Washington D.C, USA). Immunohistochemical pictures were taken using a Panoramic 250 Flash II Digital Slide Scanner and analyzed with the Panoramic Viewer (3DHISTECH Ltd., Budapest, Hungary).

Immunolabeling for ATRX was considered as positive if tumor cells had nuclear labeling, whatever its intensity (1, 2 or 3), with no evidence of cytoplasmic labeling. Neoplasms were scored as negative for ATRX if there was no labeling. One tumor presenting cytoplasmic sequestration with a strong intensity was considered as interpretable. The internal controls (inflammatory and endothelial cells) had to be positive with a nuclear labeling; otherwise the case was considered as not interpretable.

Immunofluorescence

One hundred and twenty-seven tumors from the two cohorts were analyzed on tissue microarrays. Tissues were deparaffinized in xylene and rehydrated in a series of ethanol baths. For antigen retrieval, slides were incubated in DAKO Target Retrieval Solution, pH 9 (S236784-2, DAKO, Carpinteria, CA, USA), for 20 min in a microwave oven. The primary antibodies and dilutions (dilution in DAKO REAL antibody diluent, S202230-2, DAKO, Carpinteria, CA, USA) used to study ALT were as follows: anti-PML (PG-M3, 1:200, sc-966, Santa-Cruz, Dallas, TX, USA) and anti-TERF2 antibody (1:200, HPA001907, Sigma, St Louis, MO, USA). All primary antibodies were incubated for 1h at room temperature (RT). Secondary antibodies and dilutions used were as follows: anti-Mouse Immunoglobulins/FITC (1:400, F0479, Dako, Carpinteria, CA, USA) and anti-Rabbit IgG (H+L) Alexa Fluor® 594 conjugate (1:500, A-11072, Invitrogen, Carlsbad, CA, USA). Slides were mounted with Vectashield/DAPI medium (H-1200-10, Vector Laboratories, Burlingame, CA, USA) and were then analyzed under a Nikon Eclipse 80i (Nikon, Melville, NY, USA) fluorescent microscope with appropriate filters. Pictures were captured using a Hamamatsu C4742-95 CCD camera (Hamamatsu, Hamamatsu City, Japan).

To study tryptase, tissue sections were blocked with 5% mouse serum PBS1X for 1h30 and incubated with mouse anti-tryptase antibody (1:300, ab2378, ABcam, Cambridge, UK) for 1h at RT. Then Alexa Fluor Plus 594 goat anti-mouse secondary antibody (1:400, A32742, Molecular Probes, Eugene, OR, USA) was incubated for 1h at RT. Slides were mounted using the Vectashield mounting medium plus DAPI (H-1200-10, Vector Laboratories, Burlingame, CA, USA). Images were acquired on a Zeiss Cell Observer microscope (Carl Zeiss, Oberkochen, Germany). Percentage of mast cells was assessed by counting the number of mast cells in 10 same size randomly localized regions of interest (ROI) in each tumor, divided by the

total number of cells in these ROI determined by the number of nuclei count with ImageJ 1.51u (NIH, USA).

Statistical analysis

Kaplan-Meier analysis was performed for metastasis-free survival and overall survival. To subdivide *ATRX* expression in two groups, expression was plotted for *ATRX* WT and altered cases, separately. The intersection between these two density curves was 4.45 (log2 FPKM) and 2.77 for cohort 1 and 2, respectively. Differential gene expression (DGE) analyses were performed by R package DESeq. Gene Ontology (GO) analysis was performed on these differentially expressed genes ($P < 0.05$ and fold-change > 2 or < -2), by R package GOseq. In parallel, significant genes with $P < 0.01$ were used to make a heatmap (R package ComplexHeatMap).

Cell culture

Human osteosarcoma cell line MG63 and mouse osteosarcoma cell line K7M2 (42) were cultured in DMEM (31966-021, Life Technologies, Carlsbad, CA, USA), human UPS cell line IB106 (43) was cultured in RPMI-1640 (524000-025, Life Technologies, Carlsbad, CA, USA). Both were supplied with 10% fetal bovine serum (S1810-500, Dutscher, Brumath, France) at 37°C in a humidified chamber containing 5% CO_2.

ShRNA Knockdown of ATRX expression

shRNAs constructs targeting human or mouse *ATRX* were obtained from OriGene (Rockville, MD, USA). The 28 bp human sequence was 5'- CCTTCTAACTACCAGCAGTTGATATGAG -3' and the 29 bp mouse sequence was 5'- CATCAAGTAGATGGTGTTCAGTTTATGTG -3'. A shRNA 29-mer scrambled shRNA was used as a negative control and obtained from OriGene.

Production of lentiviruses

Lentiviruses were produced by co-transfection of pVSVg, psPAX2 and shRNA construct in HEK293T cells. Co-transfection was performed by adding these plasmids, chloroquine at 0.025 mM (C6628, Sigma, St Louis, MO, USA), $CaCl_2$ at 0.125 M (C5050, Sigma, St Louis, MO, USA) and HeBS 1X (51558, Sigma, St Louis, MO, USA), HEK293T cells were then incubated at 37°C in a humidified chamber containing 5% CO_2. After 6 hours, HEK293T cell medium was changed with RPMI-1640 (524000-025, Life Technologies, Carlsbad, CA, USA) containing 10% of fetal bovine serum (S1810-500, Dutscher, Brumath, France).

Lentiviral transduction

HEK293T cell culture medium was filtered with a 0.45 µm PES filter and was mixed at 1:1 ratio with K7M2, MG63 or IB106 culture medium previously seeded. Polybrene (8 µg/ml, H9268, Sigma, St Louis, MO, USA) was also added with the virus. Infected cells were selected with puromycin and cells were sorted by FACS (BDFACSAria, BD Biosciences, San Jose, CA, USA) thanks to their GFP expression when vector with shRNA *ATRX* was integrated.

Western Blot analysis

Protein extracts were separated from each cell line with RIPA protein lysis buffer (R0278, Sigma, St Louis, MO, USA) containing 1X protease cocktail (P8340, Sigma, St Louis, MO, USA). Protein extracts were separated by electrophoresis on acrylamide gel (456-8085, Bio-Rad, Hercules, CA, USA) and transferred onto PVDF membrane. Then they were probed with antibodies against ATRX (1:1000, HPA001906, Sigma, St Louis, MO, USA) or actin (1:5000, A5316, Sigma, St Louis, MO, USA). Proteins of interest were detected with HRP-conjugated sheep anti-mouse IgG antibody (1:5000, NAX931V, GE Healthcare, Piscataway, NJ, USA) or HRP-conjugated donkey anti-rabbit IgG antibody (1:5000, GENA934V, Sigma, St Louis, MO, USA) and visualized with the ECL prime Western blotting detection regent (RPN2236, GE

Healthcare, Piscataway, NJ, USA), according to the manufacturer's recommendations and using the PXi system (Syngene, Bangalore, India).

Cell proliferation assay

Cells of each cell line with $ATRX^{KD}$ or $ATRX^{CT}$ were seeded onto a 96-well plate (3.10^3 cells/well). After 4 days, cell proliferation was evaluated by adding 20 µL of MTT (M2128, 5mg/mL, Sigma, St Louis, MO) to cell medium. Two hours later, medium was replaced by 100 µL of DMSO (5879, Sigma, St Louis, MO, USA) and the optic density (OD) of each well was read with a spectrophotometer (PowerWaveX, Bio-Tel Instrument, Winooski, VT, USA) at 570 and 630 nm. Live cell number was correlated to $\Delta OD = OD_{570nm} - OD_{630nm}$. Experiments were performed independently in triplicate three times.

Soft agar assay

Cells of each cell line with $ATRX^{KD}$ or $ATRX^{CT}$ were seeded (5000 cells/well) in 0.35 % agarose cell medium (16500-500, Invitrogen, Carlsbad, CA, USA) onto a 6-well plate containing a 0.5 % agar base. 0.5 mL of cell culture medium was added and changed every 3-4 days. After incubating for 3 to 4 weeks, colonies were visualized with 0.005 % crystal violet staining (HT90132, Sigma, St Louis, MO, USA). Experiments were performed independently in triplicate four times.

***In vivo* experimentations**

Mice were maintained under specific pathogen-free conditions in the animal facility of University of Bordeaux (France) or at the CREFRE (Centre Régional d'Exploration Fonctionnelle et Ressources Expérimentales, Toulouse, France). Experiments were performed in conformity with the rules of the Institutional Animal Care and Use committee (approval number DAP-APAFiS-2018041617309605) and all efforts were made to minimize animal suffering. For all experiments, 10^6 cells were injected into the dorsal flank of 6-8-week-old

NSG (NOD/Shi-scid/IL-2Rgammanull) mice or Balb/c mice. Tumor sizes were measured twice a week using a caliper and their volume was calculated using the formula: $l^2 \times L/2$. At the end of the experiment, mice were sacrificed by cervical dislocation. Tumors were then weighed and divided in two parts for formalin fixation and nitrogen freezing. Each tumor was stained with HE and analyzed by a pathologist specialized in sarcomas. Growth rate was calculated with the segmental linear regression of GraphPad Prism (GraphPad Software, San Diego, CA, USA) and statistical analyses were done using an unpaired T-test. Survival curves were analyzed with GraphPad Prism using the Kaplan-Meier method.

Mice tumor RNA sequencing and analysis

Total RNA was extracted, prepared and sequenced as described in supplementary methods to obtain more than 20 million paired-end reads with a length of 75 bp each. Bioinformatic analysis was done as previously described (17).

RNA reads were aligned to the mm10 genome assembly with STAR v2.6.0c (44). Low-quality (score < 20) and duplicated PCR paired-end reads were removed with SAMtools v1.8 (45) and PicardTools v2.18.2 (http://broadinstitute.github.io/picard/index.html), respectively. Then, gene expression was quantified with Cufflinks v2.2.1 (46), using RefSeq (47) genes (without miRNA and rRNA) from mm10 UCSC Table Browser (48) fixed on 2019/01.

Differential gene expression was performed by R package DESeq, between $ATRX^{KD}$ and $ATRX^{CT}$ tumors extracted from Balb/c mice. Relationships between proteins overexpressed in $ATRX^{KD}$ and $ATRX^{CT}$ tumors were assessed by the STRING Database (18).

Expression data are available on Gene Expression Omnibus (GEO) under accession GSE157953.

ALT specific c-circle detection

The C-circle assay, which partially detects single-stranded telomeric (CCCTAA)n DNA circles (C-circles) amplified by the Phi29 polymerase in the absence of dCTP, was performed as previously described (49).

Acknowledgments: The authors would like to thank the Centre Nacional d'Anàlisi Genòmica (CNAG, Barcelona, Spain) for WG and RNA sequencing services. We acknowledge the personnel of CREFRE US006 and Animal Facility A2 for their technical assistance. We thank Mickaël Michaud for his technical and theoretical advice and Michel Charbonneau and Nathalie Grandin for their work on ALT detection in cell lines. We acknowledge Françoise Redini for providing us MG63 and K7M2 cell lines.

References:

1. Blay J-Y, Soibinet P, Penel N, Bompas E, Duffaud F, Stoeckle E, et al. Improved survival using specialized multidisciplinary board in sarcoma patients. Ann Oncol. 2017;28:2852–9.
2. Serrano C, George S. Leiomyosarcoma. Hematol Oncol Clin North Am. 2013;27:957–74.
3. Nicolas MM, Tamboli P, Gomez JA, Czerniak BA. Pleomorphic and dedifferentiated leiomyosarcoma: clinicopathologic and immunohistochemical study of 41 cases. Hum Pathol. 2010;41:663–71.
4. Oda Y, Miyajima K, Kawaguchi K, Tamiya S, Oshiro Y, Hachitanda Y, et al. Pleomorphic leiomyosarcoma: clinicopathologic and immunohistochemical study with special emphasis on its distinction from ordinary leiomyosarcoma and malignant fibrous histiocytoma. Am J Surg Pathol. 2001;25:1030–8.
5. The Cancer Genome Atlas Research Network, Abeshouse A, Adebamowo C, Adebamowo SN, Akbani R, Akeredolu T, et al. Comprehensive and Integrated Genomic Characterization of Adult Soft Tissue Sarcomas. Cell. 2017;171:950-965.e28.
6. Isfort RJ, Cody DB, Lovell GJ, Gioeli D, Weissman BE, Doersen C-J. Analysis of oncogene, tumor suppressor gene, and chromosomal alterations in HeLa × osteosarcoma somatic cell hybrids. Mol Carcinog. 1999;25:30–41.
7. Calo E, Quintero-Estades JA, Danielian PS, Nedelcu S, Berman SD, Lees JA. Rb regulates fate choice and lineage commitment in vivo. Nature. 2010;466:1110–4.
8. Pérot G, Chibon F, Montero A, Lagarde P, de Thé H, Terrier P, et al. Constant p53 Pathway Inactivation in a Large Series of Soft Tissue Sarcomas with Complex Genetics. Am J Pathol. 2010;177:2080–90.

9. Rubio R, García-Castro J, Gutiérrez-Aranda I, Paramio J, Santos M, Catalina P, et al. Deficiency in p53 but not Retinoblastoma Induces the Transformation of Mesenchymal Stem Cells In vitro and Initiates Leiomyosarcoma In vivo. Cancer Res. 2010;70:4185–94.
10. Gibbons RJ, Picketts DJ, Villard L, Higgs DR. Mutations in a putative global transcriptional regulator cause X-linked mental retardation with α-thalassemia (ATR-X syndrome). Cell. 1995;80:837–45.
11. Heaphy CM, Wilde RF de, Jiao Y, Klein AP, Edil BH, Shi C, et al. Altered Telomeres in Tumors with ATRX and DAXX Mutations. Science. 2011;333:425–425.
12. Marzec P, Armenise C, Pérot G, Roumelioti F-M, Basyuk E, Gagos S, et al. Nuclear-Receptor-Mediated Telomere Insertion Leads to Genome Instability in ALT Cancers. Cell. 2015;160:913–27.
13. Liau J-Y, Tsai J-H, Jeng Y-M, Lee J-C, Hsu H-H, Yang C-Y. Leiomyosarcoma With Alternative Lengthening of Telomeres Is Associated With Aggressive Histologic Features, Loss of ATRX Expression, and Poor Clinical Outcome: Am J Surg Pathol. 2015;39:236–44.
14. Kovatcheva M, Liu DD, Dickson MA, Klein ME, O'Connor R, Wilder FO, et al. MDM2 turnover and expression of ATRX determine the choice between quiescence and senescence in response to CDK4 inhibition. Oncotarget. 2015;6:8226–43.
15. Han M, Napier CE, Frölich S, Teber E, Wong T, Noble JR, et al. Synthetic lethality of cytolytic HSV-1 in cancer cells with ATRX and PML deficiency. J Cell Sci. 2019;132.
16. Clynes D, Jelinska C, Xella B, Ayyub H, Scott C, Mitson M, et al. Suppression of the alternative lengthening of telomere pathway by the chromatin remodelling factor ATRX. Nat Commun [Internet]. 2015 [cited 2016 Jul 26];6. Available from: http://www.ncbi.nlm.nih.gov/pmc/articles/PMC4501375/
17. Lesluyes T, Pérot G, Largeau MR, Brulard C, Lagarde P, Dapremont V, et al. RNA sequencing validation of the Complexity INdex in SARComas prognostic signature. Eur J Cancer Oxf Engl 1990. 2016;57:104–11.
18. Szklarczyk D, Gable AL, Lyon D, Junge A, Wyder S, Huerta-Cepas J, et al. STRING v11: protein-protein association networks with increased coverage, supporting functional discovery in genome-wide experimental datasets. Nucleic Acids Res. 2019;47:D607–13.
19. Chudasama P, Mughal SS, Sanders MA, Hübschmann D, Chung I, Deeg KI, et al. Integrative genomic and transcriptomic analysis of leiomyosarcoma. Nat Commun [Internet]. 2018 [cited 2019 Sep 12];9. Available from: https://www.ncbi.nlm.nih.gov/pmc/articles/PMC5762758/
20. Lee PJ, Yoo NS, Hagemann IS, Pfeifer JD, Cottrell CE, Abel HJ, et al. Spectrum of mutations in leiomyosarcomas identified by clinical targeted next-generation sequencing. Exp Mol Pathol. Academic Press; 2017;102:156–61.
21. Watson LA, Goldberg H, Bérubé NG. Emerging roles of ATRX in cancer. Epigenomics. 2015;7:1365–78.

22. Ren X, Tu C, Tang Z, Ma R, Li Z. Alternative lengthening of telomeres phenotype and loss of ATRX expression in sarcomas. Oncol Lett. 2018;15:7489–96.

23. Yang C-Y, Liau J-Y, Huang W-J, Chang Y-T, Chang M-C, Lee J-C, et al. Targeted next-generation sequencing of cancer genes identified frequent TP53 and ATRX mutations in leiomyosarcoma. Am J Transl Res. 2015;7:2072–81.

24. Chen X, Bahrami A, Pappo A, Easton J, Dalton J, Hedlund E, et al. Recurrent Somatic Structural Variations Contribute to Tumorigenesis in Pediatric Osteosarcoma. Cell Rep. Cell Press; 2014;7:104–12.

25. Ahvenainen TV, Mäkinen NM, von Nandelstadh P, Vahteristo MEA, Pasanen AM, Bützow RC, et al. Loss of ATRX/DAXX expression and alternative lengthening of telomeres in uterine leiomyomas. Cancer. 2018;124:4650–6.

26. DeBerardinis RJ, Chandel NS. Fundamentals of cancer metabolism. Sci Adv [Internet]. American Association for the Advancement of Science; 2016 [cited 2020 May 26];2. Available from: http://www-ncbi-nlm-nih-gov.//pmc/articles/PMC4928883/

27. Komi DEA, Redegeld FA. Role of Mast Cells in Shaping the Tumor Microenvironment. Clin Rev Allergy Immunol [Internet]. 2019 [cited 2019 Sep 18]; Available from: https://doi.org/10.1007/s12016-019-08753-w

28. Crawford G, Hayes MD, Seoane RC, Ward S, Dalessandri T, Lai C, et al. Epithelial damage and tissue γδ T cells promote a unique tumor-protective IgE response. Nat Immunol. Europe PMC Funders; 2018;19:859.

29. Oldford SA, Haidl ID, Howatt MA, Leiva CA, Johnston B, Marshall JS. A Critical Role for Mast Cells and Mast Cell-Derived IL-6 in TLR2-Mediated Inhibition of Tumor Growth. J Immunol. American Association of Immunologists; 2010;185:7067–76.

30. Koelsche C, Renner M, Johann P, Leiss I, Sahm F, Schimmack S, et al. Differential nuclear ATRX expression in sarcomas. Histopathology. 2016;68:738–45.

31. Mitson M, Kelley LA, Sternberg MJE, Higgs DR, Gibbons RJ. Functional significance of mutations in the Snf2 domain of ATRX. Hum Mol Genet. Oxford Academic; 2011;20:2603–10.

32. Ayodele O, Abdul Razak AR. Immunotherapy in soft-tissue sarcoma. Curr Oncol [Internet]. 2020 [cited 2020 Jun 18];26. Available from: https://current-oncology.com/index.php/oncology/article/view/5407

33. D'Angelo SP, Mahoney MR, Van Tine BA, Atkins J, Milhem MM, Jahagirdar BN, et al. Nivolumab with or without ipilimumab treatment for metastatic sarcoma (Alliance A091401): two open-label, non-comparative, randomised, phase 2 trials. Lancet Oncol. 2018;19:416–26.

34. Wilky BA, Trucco MM, Subhawong TK, Florou V, Park W, Kwon D, et al. Axitinib plus pembrolizumab in patients with advanced sarcomas including alveolar soft-part sarcoma: a single-centre, single-arm, phase 2 trial. Lancet Oncol. 2019;20:837–48.

35. Robbins PF, Morgan RA, Feldman SA, Yang JC, Sherry RM, Dudley ME, et al. Tumor Regression in Patients With Metastatic Synovial Cell Sarcoma and Melanoma Using Genetically Engineered Lymphocytes Reactive With NY-ESO-1. J Clin Oncol. American Society of Clinical Oncology; 2011;29:917–24.

36. Dillman R, Barth N, Selvan S, Beutel L, de Leon C, DePriest C, et al. Phase I/II Trial of Autologous Tumor Cell Line–Derived Vaccines for Recurrent or Metastatic Sarcomas. Cancer Biother Radiopharm. Mary Ann Liebert, Inc., publishers; 2004;19:581–8.

37. Finkelstein SE, Iclozan C, Bui MM, Cotter MJ, Ramakrishnan R, Ahmed J, et al. Combination of External Beam Radiotherapy (EBRT) With Intratumoral Injection of Dendritic Cells as Neo-Adjuvant Treatment of High-Risk Soft Tissue Sarcoma Patients. Int J Radiat Oncol. 2012;82:924–32.

38. Oldford SA, Marshall JS. Mast cells as targets for immunotherapy of solid tumors. Mol Immunol. 2015;63:113–24.

39. Singer J, Jensen-Jarolim E. IgE-based immunotherapy of cancer: challenges and chances. Allergy. John Wiley & Sons, Ltd; 2014;69:137–49.

40. Teo PZ, Utz PJ, Mollick JA. Using the allergic immune system to target cancer: activity of IgE antibodies specific for human CD20 and MUC1. Cancer Immunol Immunother. 2012;61:2295–309.

41. Fletcher C, Bridge JA, Hogendoorn P, Mertens F. WHO Classification of Tumours of Soft Tissue and Bone. 4th ed. Lyon: IARC Press; 2013.

42. Khanna C, Prehn J, Yeung C, Caylor J, Tsokos M, Helman L. An orthotopic model of murine osteosarcoma with clonally related variants differing in pulmonary metastatic potential. Clin Exp Metastasis. 2000;18:261–71.

43. Lagarde P, Brulard C, Pérot G, Mauduit O, Delespaul L, Neuville A, et al. Stable Instability of Sarcoma Cell Lines Genome Despite Intra-Tumoral Heterogeneity: A Genomic and Transcriptomic Study of Sarcoma Cell Lines. Austin J Genet Genomic Res. 2015;2:1014.

44. Dobin A, Davis CA, Schlesinger F, Drenkow J, Zaleski C, Jha S, et al. STAR: ultrafast universal RNA-seq aligner. Bioinformatics. 2013;29:15–21.

45. Li H, Handsaker B, Wysoker A, Fennell T, Ruan J, Homer N, et al. The Sequence Alignment/Map format and SAMtools. Bioinformatics. 2009;25:2078–9.

46. Trapnell C, Williams BA, Pertea G, Mortazavi A, Kwan G, Baren MJ van, et al. Transcript assembly and quantification by RNA-Seq reveals unannotated transcripts and isoform switching during cell differentiation. Nat Biotechnol. 2010;28:511–5.

47. Pruitt KD, Tatusova T, Brown GR, Maglott DR. NCBI Reference Sequences (RefSeq): current status, new features and genome annotation policy. Nucleic Acids Res. 2012;40:D130–5.

48. Karolchik D, Hinrichs AS, Furey TS, Roskin KM, Sugnet CW, Haussler D, et al. The UCSC Table Browser data retrieval tool. Nucleic Acids Res. 2004;32:D493–6.

49. Fogli A, Demattei M-V, Corset L, Vaurs-Barrière C, Chautard E, Biau J, et al. Detection of the alternative lengthening of telomeres pathway in malignant gliomas for improved molecular diagnosis. J Neurooncol. 2017;135:381–90.

Figures and legends:

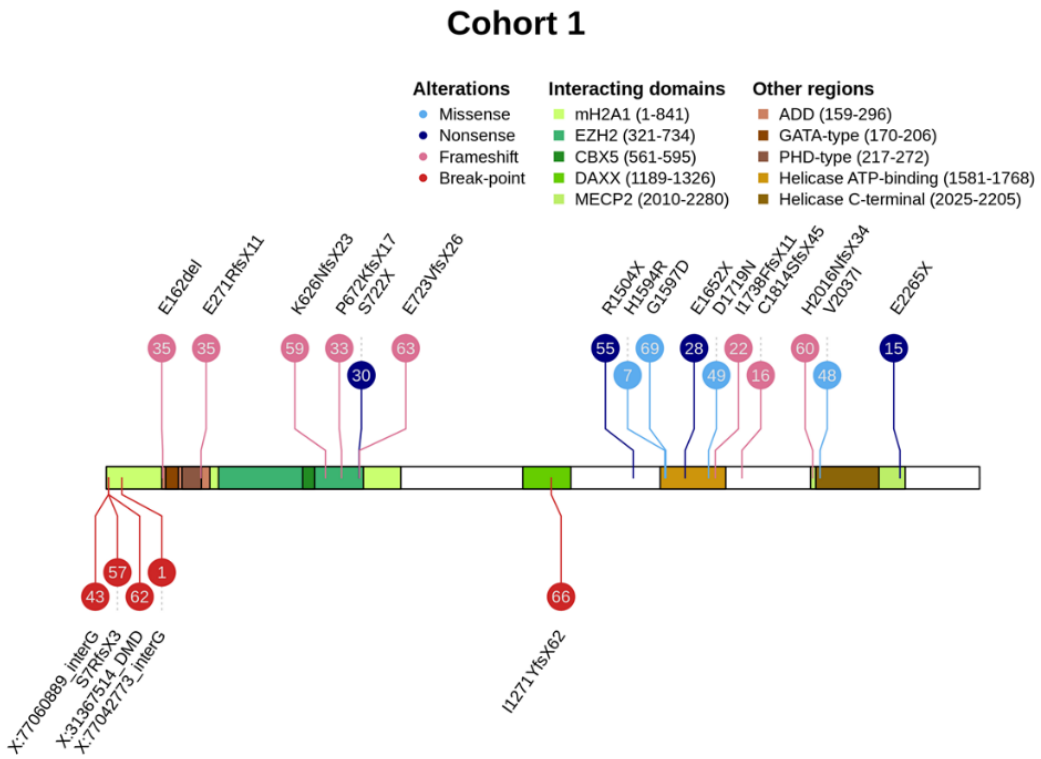

Figure 1: *ATRX* mutations and structural variants

ATRX alterations are color-coded according to their type (legend at the top). Numbers in bubbles represent tumor sample. Consequences of all point mutations on ATRX protein are annotated above a schematic representation of the protein, or below for two structural variants

(LMS57 and LMS66). For the other three structural variants, annotations correspond to the break-point partner in genomic coordinates.

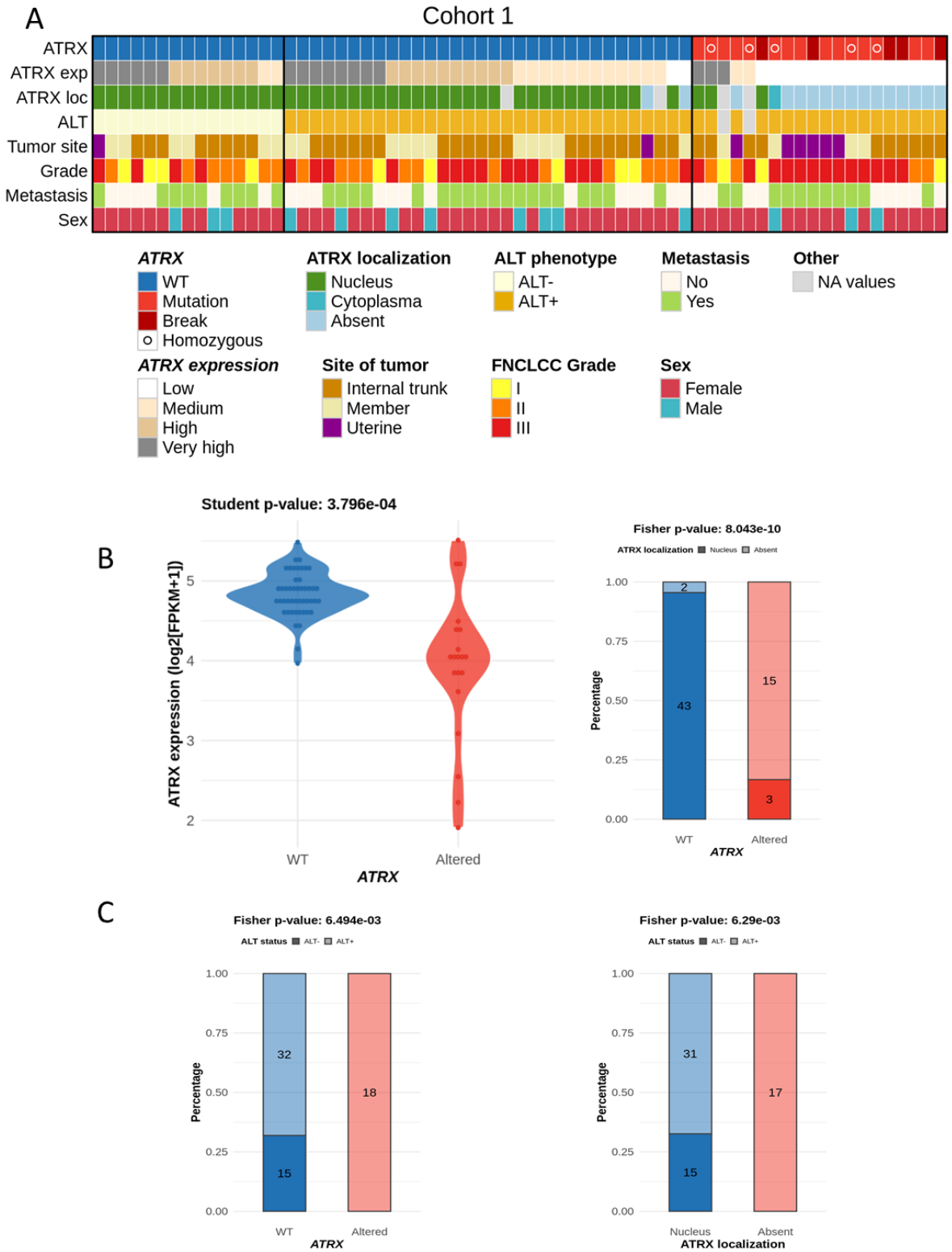

Figure 2: ATRX status and integrated representation

A Integrated representation shows *ATRX* alterations, *ATRX* mRNA expression (by quartile), ATRX localization, ALT mechanism phenotype, tumor site, FNCLCC grade, presence or not of metastasis and sex of each patient. Tumors are ordered by *ATRX* status, ALT phenotype, mRNA expression and protein localization. **B** Association between *ATRX* alteration and its mRNA expression (log2(FPKM+1)) (left) or its protein localization (right). **C** Relation between *ATRX* status (left) or its protein localization (right) and ALT mechanism phenotype. For ATRX localization, the "absent" group means "not at the nucleus", including all cases without expression and the case with a cytoplasmic localization (LMS16). P-values were calculated with Student test for **B - left** and with Fisher test for **B - right** and **C**.

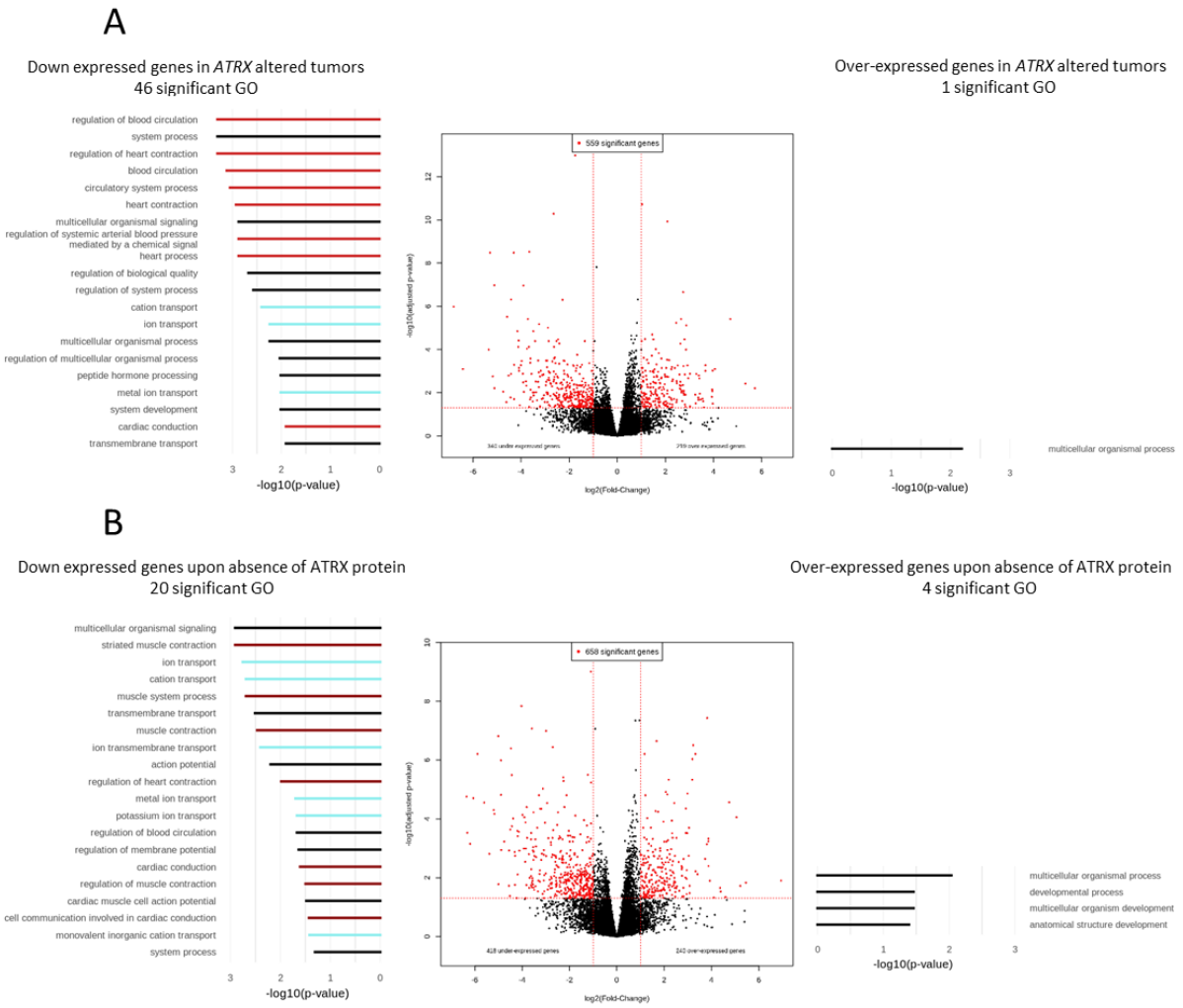

Figure 3: Differential gene expression and Gene Ontology analyses according to ATRX alteration in leiomyosarcomas (Cohort 1)

Differentially expressed genes according to **A** *ATRX* status (wild-type *vs* altered) or **B** ATRX expression (nucleus *vs* absent). Red dots indicate significant genes ($P \leq 0.05$ and fold-change ≤ -2 or ≥ 2). Gene Ontology (GO) analyses, represented on the left (under-expressed genes) and the right (over-expressed genes), identified 46 and 1 significant GO terms ($P \leq 0.05$), respectively in **A** and 20 and 4 significant GO terms ($P \leq 0.05$) in **B**. On each side, the 20 most significant GO terms are represented and color-coded by mechanisms; light red, dark red, light blue and black colors indicate "circulatory system process", "muscle system process", "ion transport" and general terms, respectively. For ATRX localization, the "absent" group means "not at the nucleus", including all cases without expression and the case with a cytoplasmic localization (LMS16). All p-values adjusted by Benjamini and Hochberg method.

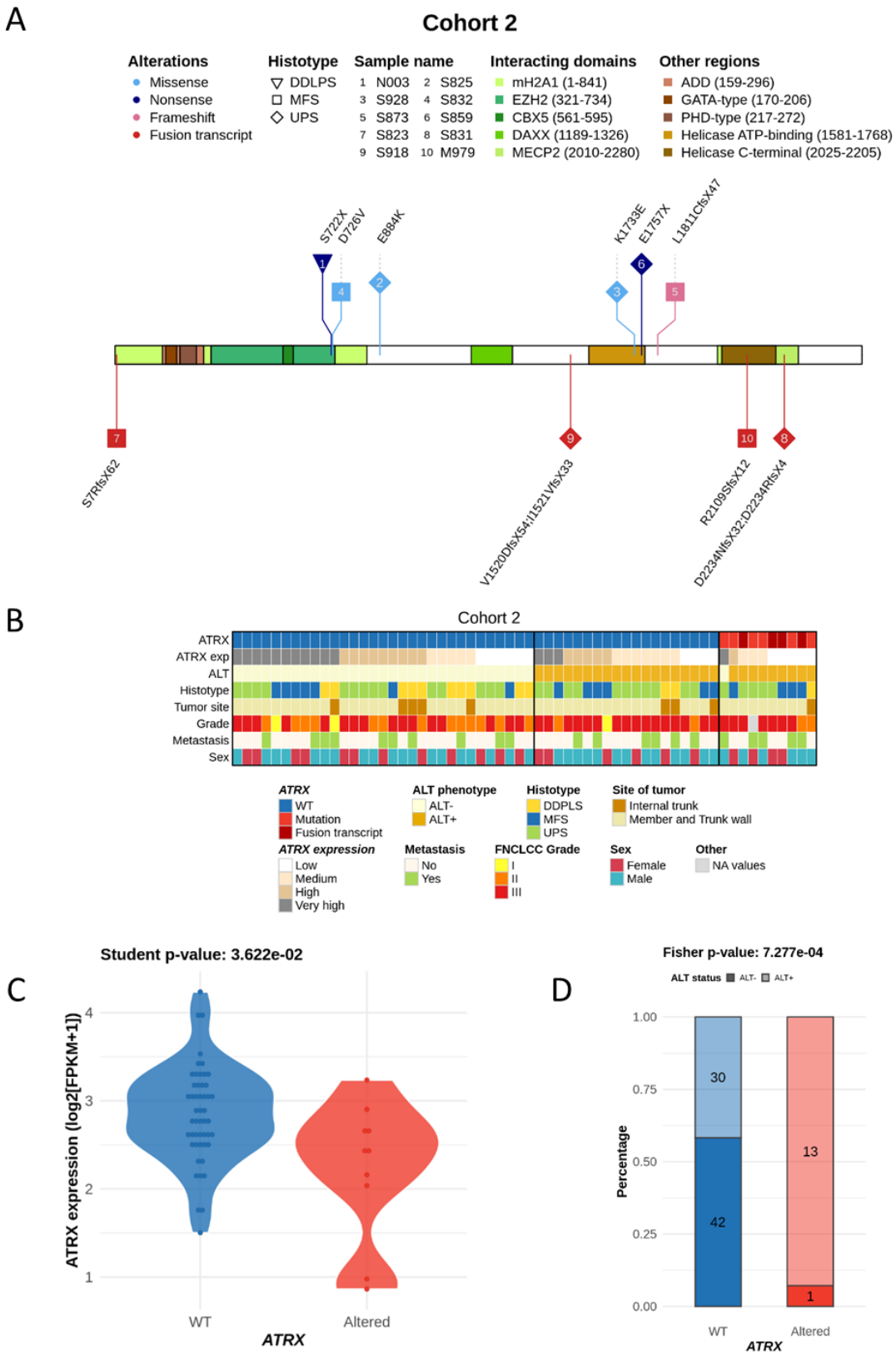

Figure 4: *ATRX* alterations and integrated representation in poorly differentiated pleomorphic sarcomas (cohort 2)

A *ATRX* alterations are color-coded by their type and shapes represent histotypes. Numbers in bubbles indicate a tumor sample (legend at the top). Translated consequences on ATRX protein is annotated above a protein schematic representation for mutations, or below for fusion transcripts. **B** Integrated representation shows *ATRX* alterations, mRNA expression (by quartile), ALT mechanism phenotype, histotypes, tumor site, FNCLCC grade, presence or not of metastasis and sex of each patient. Tumors are ordered by *ATRX* status, ALT phenotype, mRNA expression and histotypes. **C** Association between *ATRX* status and its mRNA expression (log2(FPKM+1)). **D** Relation between *ATRX* status and ALT phenotype.

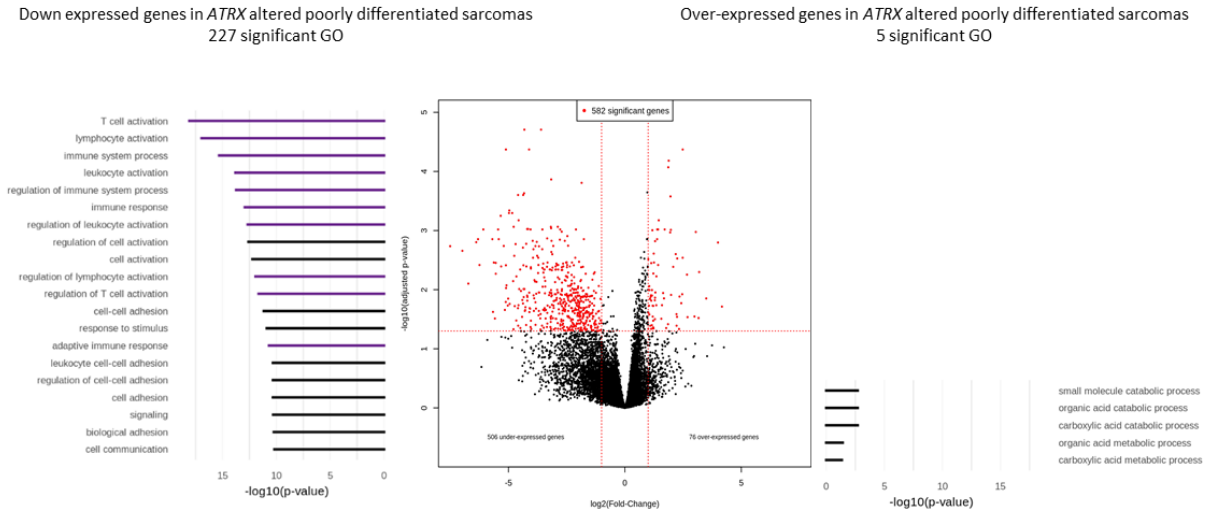

Figure 5: Differential gene expression and Gene Ontology analyses according to *ATRX* status (wild-type *vs* altered) in poorly differentiated sarcomas (Cohort 2)

Differentially expressed genes in *ATRX*-altered tumors are represented in red ($P \leq 0.05$ and fold-change $\leq$ -2 or $\geq$ 2). Gene Ontology (GO) analyses, represented on the left (under-expressed genes) and the right (over-expressed genes), identified 227 and 5 significant GO terms ($P \leq 0.05$), respectively. On the left, the 20 most significant GO terms are represented and color-coded by mechanism; purple and black groups indicate "immunity system process" and general terms, respectively. All p-values adjusted by Benjamini and Hochberg method.

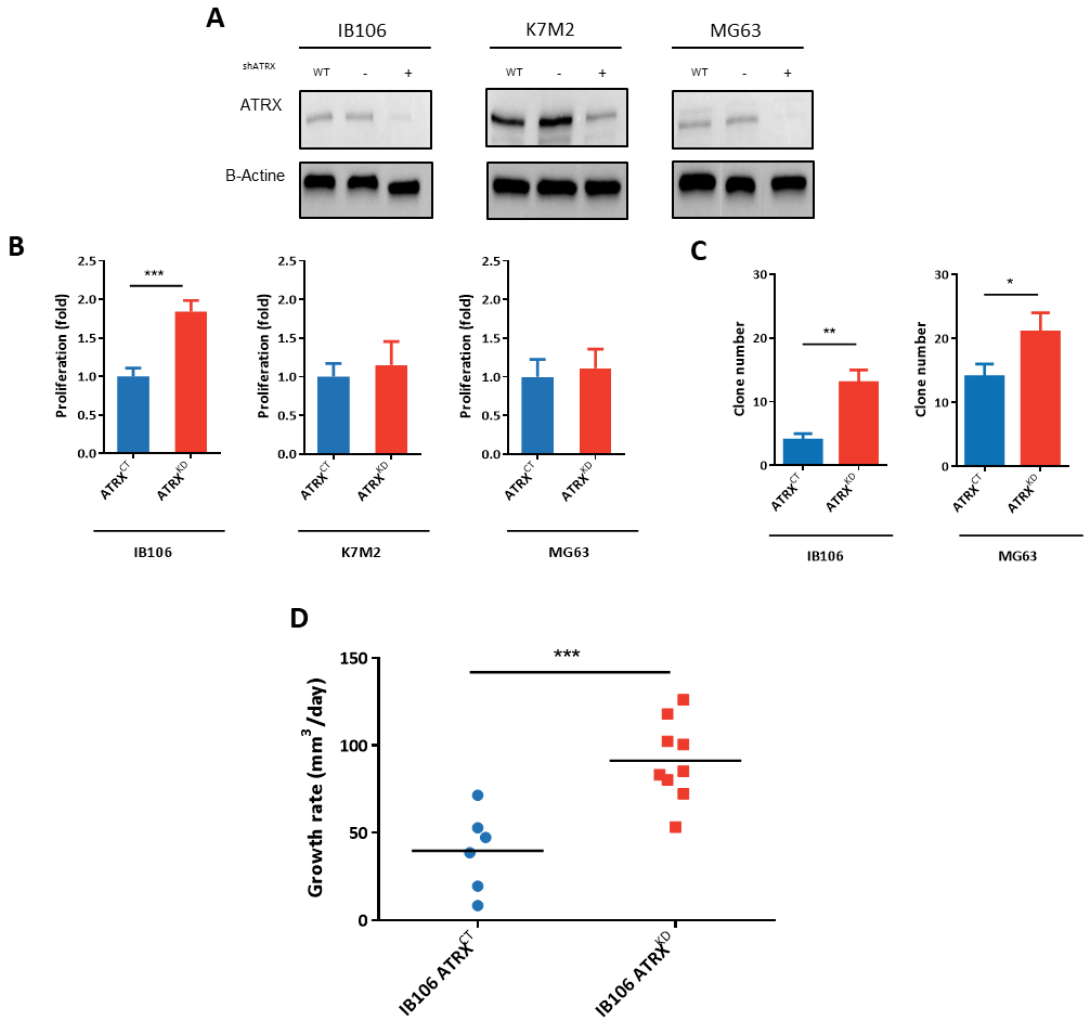

Figure 6: *ATRX* knock-down increases aggressiveness of sarcoma cells

A *ATRX* knock-down by shRNA validation in western blot in K7M2, MG63 and IB106 cell lines. **B** Proliferation analysis by MTT after 4 days, comparing $ATRX^{CT}$ and $ATRX^{KD}$ cells in K7M2, MG63 and IB106 cell lines (mean ± s.d.; n = 3 independent experiments). **C** Soft agar assay analysis comparing $ATRX^{CT}$ and $ATRX^{KD}$ cells in K7M2, MG63 and IB106 cell lines (mean ± s.d.; n = 4 independent experiments). Images were taken after 4 weeks and crystal violet staining. **D** Tumor growth rate analysis of IB106 $ATRX^{CT}$ or IB106 $ATRX^{KD}$ cells sub-cutaneous xenografts on NSG mice (N = 10 in each group). Growth rate is calculated by segmental linear regression with GraphPad. $*P \leq 0.05$, $**P \leq 0.01$, $***P \leq 0.001$, p-value was calculated with 2-way ANOVA for A and unpaired t-test for B, C and D.

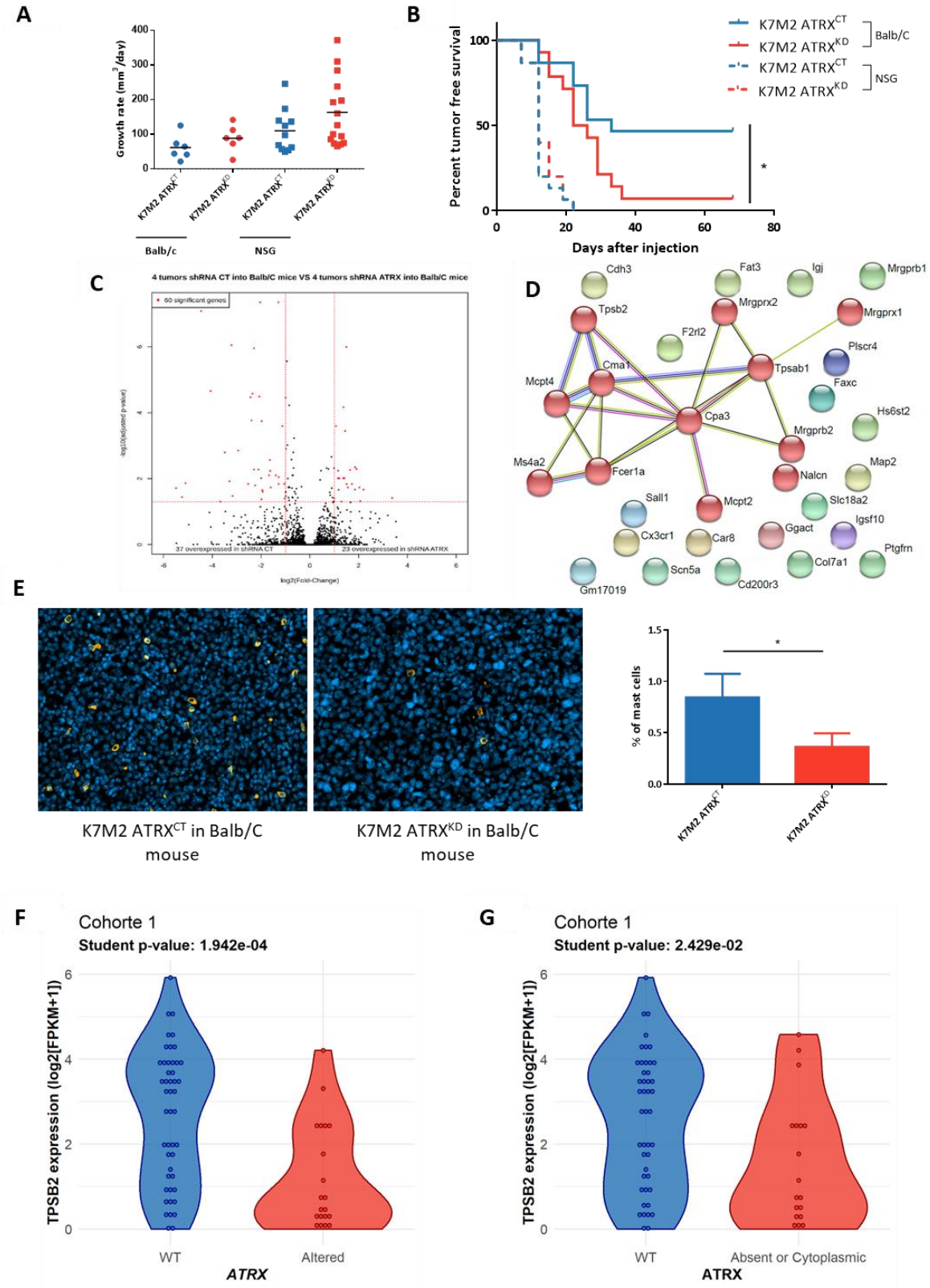

Figure 7: *ATRX* knock-down allows immune escape of sarcomas *via* non-recruitment of mast cells

A Tumor growth rate analysis of K7M2 *ATRX*^{CT} or K7M2 *ATRX*^{KD} cells xenografted under the skin of NSG or Balb/c mice (N = 15 in each group). **B** Tumor-free survival curves of K7M2 *ATRX*^{CT} or *ATRX*^{KD} tumors in immunodeficient NSG mice and immunocompetent Balb/c mice (N = 15 mice for each condition) using Kaplan-Meier method. **C** Comparison of RNA expression in log2(FPKM+1) of K7M2 *ATRX*^{KD} tumors *versus* K7M2 *ATRX*^{CT} tumors developed in immunocompetent mice (N=4 each) showing 23 and 37 significantly up- and down-expressed genes in K7M2 *ATRX*^{KD} tumors, respectively. **D** Links between down-expressed genes in K7M2 *ATRX*^{KD} tumors found by the STRING Database showing one cluster with genes involved in mast cells *via* MCL clustering. **E** Immunostaining of mast cells by targeting tryptase in K7M2 *ATRX*^{CT} and K7M2 *ATRX*^{KD} tumor tissues with nucleus marked with DAPI. On the right, percent of mast cells in the two conditions. **F** TPSB2 mRNA expression in log2(FPKM+1) according to *ATRX* status in cohort 1. **G** TPSB2 mRNA expression in log2(FPKM+1) according to ATRX localization in cohort 1. *$P \leq 0.05$, **$P \leq 0.01$, ***$P \leq 0.001$, p-value was calculated with Mantel-Cox test for B and unpaired t-test for E, F, G.